# Electron Bernstein Wave Studies in MAST

V. Shevchenko[1], G. Cunningham[1], A. Gurchenko[2], E. Gusakov[2], B. Lloyd[1], M. O'Brien[1], A. Saveliev[2], A. Surkov[2], F.Volpe[3], M. Walsh[1]

[1]*EURATOM/UKAEA Fusion Association, Culham Science Centre, Abingdon, Oxon, OX14 3DB, UK*
[2]*Ioffe Institute, Politekhnicheskaya 26, 194021 St. Petersburg, Russia*
[3]*General Atomics, P.O. Box 85608, San Diego, California 92186-5608, USA*

**Abstract.** There is a comprehensive, closely-interlinked electron Bernstein wave (EBW) programme on MAST covering heating experiments, plasma start-up studies, plasma emission measurements, theory and modelling. In this paper we report on proof-of-principle EBW heating experiments conducted on MAST with a 60 GHz, 1 MW gyrotron complex. A 28 GHz (200 kW) EBW start-up system has been commissioned on MAST. The system is capable of launching both the X-mode and O-mode. The launched O-mode is mode converted into the X-mode by a mirror-polariser incorporated in a graphite tile on the centre column. As a result the X-mode is incident on the plasma from the high field side allowing efficient EBW excitation during the plasma start-up phase. First experimental results on non-inductive plasma current generation are presented. A frequency scanning EBW radiometer has been upgraded with a fast spinning mirror and 12 parallel receiving channels covering the range of 6-18 GHz. This system allows real time measurements of mode conversion dynamics during plasma evolution. First test results are presented.

**Keywords:** EBW, plasma heating, current drive, EBW emission, plasma start-up.
**PACS:** 52.25.Os, 52.55.Wq, 52.35.Hr, 52.50.-b

## INTRODUCTION

Conventional ECRH and ECCD methods typically cannot be used in spherical tokamaks (STs) because of the specific plasma parameters. Usually the plasma is well overdense in STs, i.e. ($\omega_{pe} >> \omega_{ce}$) where $\omega_{ce}$ and $\omega_{pe}$ are the electron cyclotron and plasma frequencies. In such plasmas the first few EC harmonics in the core plasma are completely obscured by the O and X mode cutoffs. In contrast, electron Bernstein waves (EBWs) can propagate in overdense plasma and may provide efficient off-axis heating and current drive (CD) in high density ST plasmas. EBWs may also be used in the plasma start-up phase due to the fact that EBW absorption and CD efficiency remain high even in relatively cold plasmas. EBWs can be excited within the plasma with the externally launched X or O modes via mode conversion mechanisms.

One of the main objectives of the Mega Amp Spherical Tokamak (MAST) programme is to explore the potential of the ST concept as a basis of a fusion Component Test Facility and a high beta fusion power plant [1]. Burning plasma STs rely on off-axis CD and start-up techniques which do not require a central solenoid. EBWs are a promising means of off-axis plasma heating and CD in STs. Following

CP933, *Radio Frequency Power in Plasmas,* edited by P. M. Ryan and D. A. Rasmussen
2007 American Institute of Physics 978-0-7354-0444-1/07/$23.00

successful demonstration of EBW CD at Culham in the COMPASS-D tokamak, by exploiting extraordinary-Bernstein (X-B) mode conversion with the X-mode launched from the high field side (HFS) [2], with efficiency $\eta_{20} = n_{e20} I_{rf} R P_{rf}^{-1} \sim 0.035$ AW$^{-1}$m$^{-2}$, exceeding that achievable with conventional ECRH for similar plasma parameters, EBW heating experiments have continued on MAST using the existing 60 GHz gyrotrons.

Extensive ray tracing modelling and thermal EBW emission (16 - 67 GHz) measurements suggest the preferable operating frequency for efficient EBW heating and CD must be in the range of the fundamental EC resonance or its lower harmonics [3, 4]. For MAST, this requires a high power RF source in the range of 16 – 30 GHz, and so an EBW CD system in this range is presently under consideration for future implementation on MAST. The present 60 GHz (~1 MW) gyrotron complex is equipped with a steerable 7 beam launching system. Despite the fact that the operating frequency is far from optimum, a number of physical processes can be studied with the existing experimental set-up.

## PROOF-OF-PRINCIPLE EBW HEATING EXPERIMENTS

The experiments were conducted at 60 GHz with injected RF power up to 0.8 MW. The first stage of the ordinary-extraordinary-Bernstein (O-X-B) mode conversion process occurs in the $\omega_{RF} = \omega_{pe}$ layer and it requires the O mode to be launched within a narrow range of angles, the so called mode conversion "window", with respect to the edge magnetic field. The angular width of this "window" depends mainly on the local density gradient length-scale. Thus, high density plasma with a steep density gradient at $n_e = 4.5 \cdot 10^{19}$m$^{-3}$ is needed for the 60 GHz experiments. This constraint requires plasmas close to the limit of MAST operational space. Therefore three different plasma scenarios have been developed especially for these experiments [5, 6].

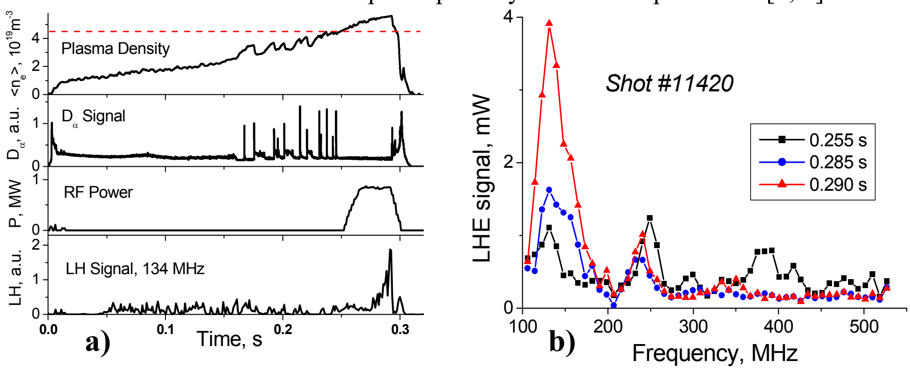


**FIGURE 1.** **a)** Line averaged plasma density, $D_\alpha$ signal and RF power in 60 GHz EBW heating experiment with ELM-free H-mode. The plasma becomes overdense i.e. the mode conversion becomes possible when plasma density is above the red dashed line. Note the strongly increased LH signal peaked at 134 MHz during the RF pulse when the plasma reached the overdense state. The probe position is about 5 cm outside the last closed flux surface. **b)** LH emission spectra during the RF pulse.

The first scenario is based on the high density ELM-free H-mode. It offers a relatively broad (±5$^{o}$) O-X-B mode conversion window due to a high density gradient in the conversion zone but EBW absorption, as predicted by modeling, is expected to be localized near r/a ~ 0.9. As the O-X-B mode conversion occurs in relatively cold plasma layers close to the separatrix, non-linear phenomena were anticipated in this scenario [7, 8]. RF power is expected to be deposited at high EC harmonics (between $5\omega_{ce}$ and $6\omega_{ce}$) leading to peripheral absorption and ineffective heating. Nevertheless, there was clear evidence of the mode conversion process as parametric decay waves originating from the UHR were observed using a specially designed lower hybrid (LH) probe. Fig. 1a illustrates a strong plasma emission enhancement around 134 MHz during the RF pulse when the plasma reached the overdense state.

The enhanced emission is localized in frequency (Fig. 1b). Due to the fact that the spectral maximum is close to the LH resonance frequency in the UHR region for 60 GHz we identify this radiation as generated by a parametric decay instability occurring in the UHR. The parametric decay requires a threshold RF power density at the UHR. This allows us to conclude that the coupling to EBW was no less than 50% in at least one of the beams [5, 6].

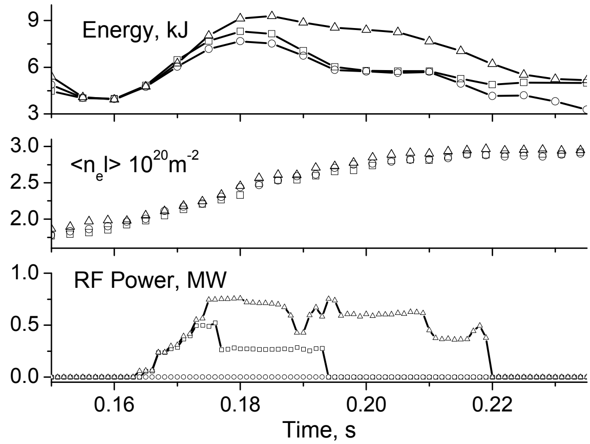


**FIGURE 2.** Plasma energy increase in Ohmic H-mode plasma during RF injection.

The second scenario is based on a sawtoothing H-mode plasma, in which a high density gradient zone allowing the O-X-B conversion appears deeper into the plasma. In this scenario the density gradient scale length is very short for pedestal densities up to $2\cdot10^{19}m^{-3}$ and has a relatively moderate value at higher densities. This allows us to shift the O-X conversion layer by 10-15 cm deeper into the plasma, avoiding interception by higher EC harmonics. As a result the mode conversion window is narrower ($\pm3^o$) in this case but the EBW power deposition can reach as far in as r/a ~ 0.6. After careful optimization of the toroidal field and launch angles a ~10% increase of the total plasma energy has been observed during RF injection.

In the third scenario, high density ohmic H-mode is achieved by plasma compression in major radius. Because plasma is compressed into a higher magnetic field, r/a ~ 0.4 becomes accessible transiently at $3\omega_{ce}$ and then at $2\omega_{ce}$ during the compression process. The mode conversion window ($\pm1.5^o$) is very restrictive in this case hence the thermal EBW plasma emission was used for the launch optimization.

EBW heating effects can be seen from the total plasma energy behaviour during RF injection, as illustrated in Fig. 2. Here three plasma shots with similar parameters are compared: one without RF injection and the other two with RF injection of different power and RF pulse duration. One can see a well pronounced (up to 30%) increase of the total plasma energy in the case of ~600 kW RF injection.

## 28 GHZ START-UP SYSTEM

It has been shown experimentally that EBW CD excited with the X-mode launched from the HFS is capable of producing a substantial amount of current [2], which could possibly sustain plasma stability during the plasma current flat top. A non-inductive plasma current start-up scenario based on EBW CD at 28 GHz has been proposed for MAST [9]. This scheme relies on the production of low-density plasma by RF pre-ionisation around the fundamental electron cyclotron resonance layer. Then a double mode conversion scheme is considered for EBW excitation in plasmas with densities lower than the O-mode cut-off density. The scheme consists of the conversion of the O-mode, incident from the low field side of the tokamak, into the X-mode with the help of a grooved mirror-polariser incorporated in a graphite tile on the central column. The X-mode reflected from the polariser propagates back to the plasma and experiences a subsequent X-EBW mode conversion near the upper hybrid resonance. Finally the excited EBW mode is totally absorbed before it reaches the EC resonance, due to the Doppler shift. The absorption of EBW remains high even in cold plasma. Furthermore, EBW can generate significant plasma current during the plasma start-up phase giving the prospect of a fully non-inductive plasma start-up scenario.

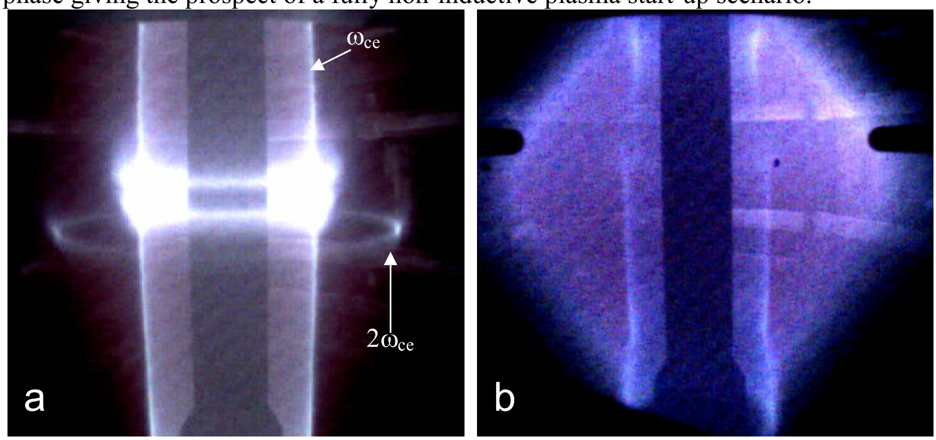


**FIGURE 3.** 28 GHz RF breakdown in the toroidal (85 kA) and 1 mT vertical magnetic field. **a)** X-mode launch, Ip ≈ 0 kA. Fundamental and second harmonic resonances are clearly visible. **b)** O-mode launch, Ip ≈ 15 kA. Plasma forms a tokamak-like shape.

The 28 GHz start-up system has now been commissioned on MAST. The gyrotron is capable of delivering up to 200 kW for 40 ms. Low-power tests were conducted using a full scale assembly of the launcher before high power injection into the MAST vessel. The RF beam pattern measured at the graphite tile shows that the beam is very close to Gaussian and 98% of the power is well within the grooved area of the mirror-polariser.

First experiments with the 28 GHz gyrotron have demonstrated a reliable preionasation with both the X-mode and the O-mode launched (see Fig. 3). Plasma currents up to 15 kA have been observed during RF breakdown without the use of solenoid flux. That was achieved with 100 kW RF injection and vertical field ($B_V$) ramp-up. However, the plasma current generated by this method could not be sustained for longer than 50 ms. After reaching the maximum value the plasma current decays slowly to zero regardless of the further $B_V$ ramp-up and RF power injection.

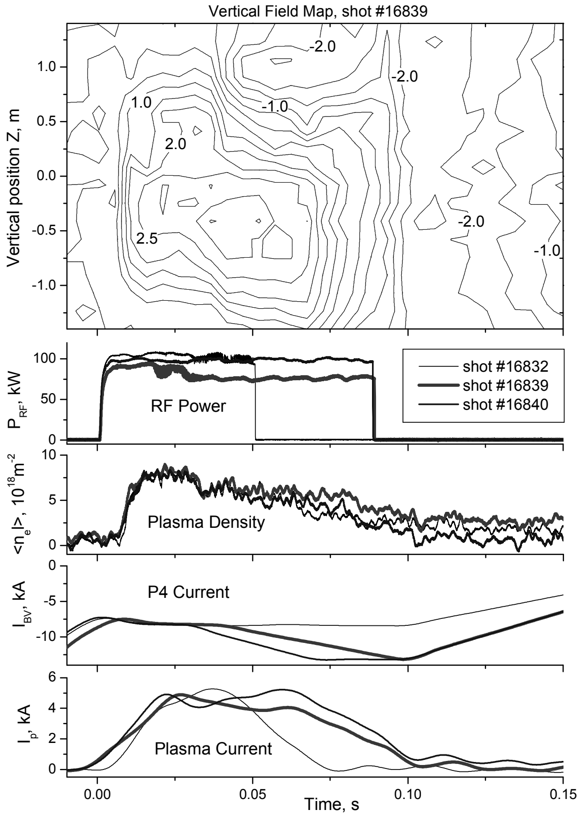


**FIGURE 4.** Plasma current generation during RF injection at constant $B_V$. O-mode injection.

To investigate this phenomenon a number of shots have been fired at constant $B_V$ during RF breakdown. Data analysis is much simpler at constant $B_V$ while the plasma behaviour seems to be the same. The plasma current reaches a 5 kA maximum in this case but then decays to zero in the same manner as with the $B_V$ ramp-up applied. Fig. 4 shows 3 shots with constant $B_V$ during the RF pulse and with further $B_V$ ramp-ups. It is clear that $B_V$ ramp-up can help to extend plasma current for another 15-20 ms but then it decays to zero. The contour map in Fig. 4 represents the vertical component of the magnetic field measured on the surface of the central rod. An offset of -2 mT has been subtracted from these signals at the beginning of the shot. The positive contours represent a positive magnetic field (up to 3 mT) produced by plasma current flowing in the positive direction. The negative contours represent negative currents flowing in the plasma and external vertical field. After the end of the RF pulse plasma currents disappear and the negative contours correspond to the maximum negative $B_V$ (-2 mT) reached at this moment.

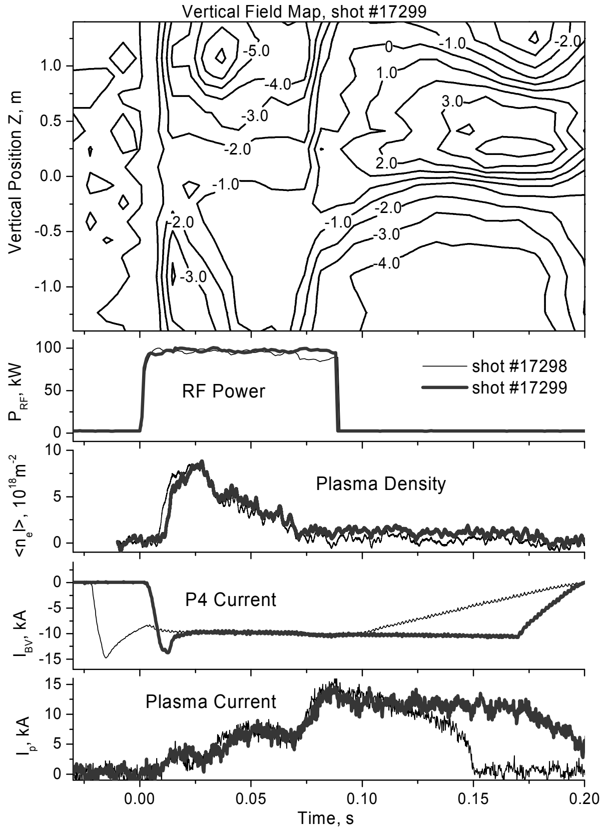


**FIGURE 5.** Plasma current generation during RF injection in vertically shifted (~25 cm) plasma at constant $B_V$. O-mode injection.

During the first 35 ms plasma current is centred near the midplane and it is positive. Then after 40 ms a significant negative current develops in the upper part of the plasma. These opposite currents repel each other and cause plasma expansion in the vertical direction. Finally these currents cancel each other and degrade the plasma.

According to our understanding the positive plasma current is generated by means of the asymmetric confinement and pressure driven currents induced by RF ionisation [10]. The negative current is predominantly due to the EBW CD mechanism. It appears later when plasma becomes relatively hot and rarefied near the resonance to provide high enough CD efficiency. The EBW CD is in a counter direction at this time due to the fact that during this phase the external $B_V$ is predominant over the plasma current field. The external $B_V$ has an opposite curvature at the UHR providing the counter direction for EBW CD. To test this hypothesis it was suggested to shift the plasma centre upwards in order to provide the right curvature of the magnetic flux in the mode conversion zone. Fig. 5 illustrates RF star-up at constant $B_V$ with the $B_V$

minimum shifted by ~25 cm above the midplane. The contour map of the $B_V$ component shows a positive current developing from the beginning of the RF injection. Plasma current is gradually rising up to the end of RF pulse and remains for some time afterwards. There are 3 distinctive reproducible ramps on the plasma current in this scenario. First there is a fast ramp up to 3-4 kA during first 10 ms. Then a small negative current (-5 mT contours) appears due to EBW CD in the upper part of the plasma. The plasma current is doubled after its disappearance at 20 ms. During this phase the plasma centre is strongly downshifted possibly due to repulsion with the negative current in the upper part. Finally EBW CD becomes positive near the midplane and causes the final current ramp up to 15 kA. The last ramp doesn't actually reach saturation, possibly with longer RF pulse the higher currents can be achieved.

## EBW RADIOMETER UPGRADE

Thermal EBW emission measurements in the frequency range 16-67 GHz covering the first 6 EC harmonics provide an important insight into the mode coupling physics [3, 6]. A frequency scanning radiometer has been upgraded with a fast spinning mirror and 12 parallel receiving channels covering the range of 6-18 GHz. The spinning mirror was installed at about $45^o$ in front of the receiving antenna of the frequency scanning EBW radiometer. This allows real time measurements of mode conversion dynamics during plasma evolution [11].

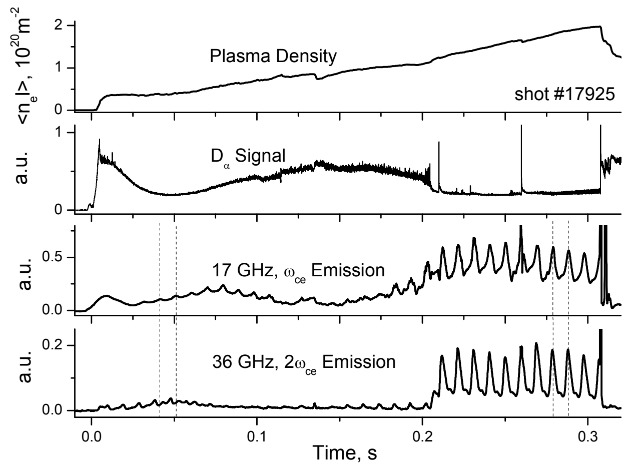


**FIGURE 6.** Thermal plasma EBW emission as measured by the frequency scanning radiometer with the fast spinning mirror. Note EBW emission enhancement during H-mode.

By design the spinning mirror can reach a maximum speed of 12 000 revolutions per minute (rpm), which gives a full angular scan every 5 ms. Radiometer signals at the spinning speed of 6 000 rpm are shown in Fig. 6. The mirror has an inclination angle of $4.5^o$, which means the angular scan is described by an elliptical cone with the $\pm 4.5^o$ vertical and $\pm 9^o$ horizontal span around the chosen viewing angle. The first results confirm that thermal EC emission from the plasma is highly anisotropic. The amplitude modulation with the period of the mirror rotation is clearly seen throughout the plasma shot at all frequencies. The vertical dashed lines indicate the maximum viewing angles in the toroidal direction. Note the modulation of $\omega_{ce}$ and $2\omega_{ce}$ signals is not in-phase during the period indicated by the first pair of lines while the signals are in-phase at the end of the shot. This illustrates that the resultant signal modulation is a combination of a number of factors: geometric modulation, the presence of stray radiation and finally anisotropic EC and EBW emission. First results are consistent in general with the previous shot-by-shot observations and theoretical predictions.

## CONCLUSIONS

Proof-of-principle EBW heating experiments have been conducted on MAST using 3 special plasma scenarios. Parametric decay instability has been observed in high density ELM-free H-mode plasmas indicating that the O-X-B mode coupling efficiency was at least 50 % in this scenario. In sawtoothing H-mode plasmas a 10% increase of plasma energy was measured during RF injection. In small ohmic H-mode plasmas a 30% increase of plasma energy due to RF heating was measured. EBW heating has therefore clearly been observed in MAST via the O-X-B mode conversion.

A 28 GHz plasma start-up system has produced reliable pre-ionization with both X-mode and O-mode launch. It was shown that with the O-mode launch, plasma currents up to 15 kA can be generated and sustained non-inductively.

First tests of the frequency scanning radiometer in combination with the fast spinning mirror have confirmed that thermal EC emission from the plasma is highly anisotropic and it exhibits fast variations throughout the plasma shot. These measurements provide an important tool for EBW coupling optimisation.

## ACKNOWLEDGMENTS

This work was funded jointly by the United Kingdom Engineering and Physical Sciences Research Council and by the European Communities under the contract of association between EURATOM and UKAEA. The views and opinions expressed in this paper do not necessarily reflect those of the European Commission.

## REFERENCES

1. B. Lloyd, in *Proc. 21st IAEA Conference*, Chengdu, 16-21 October 2006, OV/2-3
2. V. Shevchenko et al., *Phys. Rev. Lett*. **89**, 265005 (2002)
3. V. Shevchenko et al., in *Proc. EC-13 Joint Workshop*, Nizhny Novgorod, Russia, p. 162, (2004)
4. G. Taylor et al., *Physics of Plasmas*, **11**, No 10, p. 4733 (2004)
5. V. Shevchenko et al., in *Proc. EC-14 Joint Workshop*, Santorini, Greece, p. 54, (2006)
6. V. Shevchenko et al., *Fusion Science and Technology* **52**, Aug (2007) to be published
7. F.C. McDermott et al., *Phys. Fluids*, **25**, No 9, p. 1488 (1982)
8. H.P. Laqua et al., *Phys. Rev. Lett*. **78**, 18, 3467 (1997)
9. V. Shevchenko et al., in *Proc. EC-13 Joint Workshop*, Nizhny Novgorod, Russia, p. 255, (2004)
10. T. Yoshinaga et al., *Phys. Rev. Lett*. **96**, 125005 (2006)
11. F. Volpe, B-27, this Conference